Coordinated scheduling based on automatic neighbor beam relation

Marie Masson, Zwi Altman, Eitan Altman

HAL Id: hal-02566350
https://inria.hal.science/hal-02566350v2

Submitted on 13 May 2020

Coordinated scheduling based on automatic neighbor beam relation

Marie Masson*, Zwi Altman* and Eitan Altman†‡
*Orange Labs
44 Avenue de la Republique, 92320 Chatillon, France
Email:{marie.masson,zwi.altman}@orange.com
†INRIA Sophia Antipolis and LINCS, France
Email:Eitan.Altman@sophia.inria.fr
‡Avignon University

Abstract—We consider a network with Massive Multiple Input Multiple Output (M-MIMO) base stations using a Grid of Beams (GoB) for data and control channels. 5G allows to establish interference relations between beams of neighboring cells. Such relations can be used to automatically generate a beam relation matrix, denoted as Automatic Neighbor Beam Relation (ANBR) matrix that can be very useful for optimizing different resource allocation processes. This paper shows how the ANBR matrix can be used to coordinate scheduling of neighboring cells with a small amount of information exchange. The coordination is performed by judicially muting or reducing the bandwidth of certain beams in the process of Multi-User (MU) Proportional Fair (PF) scheduling. Numerical results show how the coordination approach can bring about significant performance gain.

Index Terms—Beam relations, ANBR, Massive MIMO, Coordination, Multi-user scheduling, Interference management, 5G

I. INTRODUCTION

M-MIMO is among the pillars of 5G technology that allows to significantly improve user rates, system capacity and Energy Efficiency (EE) [1]. The concept of GoB has been introduced to allow beamforming of control channels that are used among others to transmit synchronization signals and to broadcast system information to allow initial access and mobility procedures [2]. Beam sweeping is used in conjunction with GoB by switched rapidly the beams one by one in a manner to cover the entire cell surface. Similarly, data channels can be transmitted using the beams of the GoB. In this case the GoB can be seen as a predefined codebook of beams that can be selected by a MU scheduler to serve users.

Beam management is an important feature introduced in 3rd Generation Partnership Project (3GPP) for 5G networks. It is part of the New Radio (NR) Automatic Neighbor Relation (ANR) and is considered as a central Self-Organizing Network (SON) function. NR ANR allows to automatically establish different types of relations involving gNodeBs (gNBs) and/or beams [3]: (i) gNB to gNB relations that consist of establishing connectivity over the Xn interface between neighboring gNBs. Such relations are necessary to support mobility, load and traffic sharing or multi-connectivity and were already standardized for 4G networks [4]; (ii) gNBs to Beam relations; and (iii) beam to beam relations, intra- and inter-cell.

The feature of automatically establishing relations between beams is denoted as ANBR. The association of user traffic and Quality of Service (QoS) information with the ANBR feedback in relation with the GoB enable the exploitation of the beam level spatial resolution to further optimize resource management functions.

This paper investigates the use of ANBR to optimize MU-Multiple Input Multiple Output (MIMO) scheduling. We assume that the ANBR feature is available and provides a binary static matrix, denoted as *ANBR matrix*, with non-zero elements representing beam relations. The way to define relations between beams is not standardized. It can be derived as in classical ANR, e.g. by calculating the average interference users of beam i experience from beam j of a neighboring cell during a long period of time, and comparing it to a predefined threshold. We show how the ANBR matrix can be used to coordinate the MU schedulers of neighboring cells in a manner to minimize collisions between potentially interfering beams, while taking into account the dynamics of the traffic.

Traditional approaches for collaboration between adjacent cells with M-MIMO deployment such as Coordinated Multipoint transmission (CoMP) [5] require signaling and computation in both the PHY and the MAC layer and are thus demanding an intensive signal processing and the exchange of important amount of information. They also have strict requirements on

the back-haul capacity. In the proposed approach, the coordination is performed at the MAC level and requires little information echange and processing power.

The paper is organized as follows. Section II presents the system model. Section III develops a coordinated MU scheduling solution relying on the ANBR. The architecture supporting the solution is also described. Numerical results are presented in Section IV followed by concluding remarks in Section V.

II. SYSTEM MODEL

Consider a hexagonal network with tri-sectoral sites, each with M-MIMO system in the Down Link (DL). GoB with beam sweeping is used for initial access (to attach users to the Base Station (BS)) and synchronization. Data transmissions use the (fixed) beams of the GoB, and the choice of users being served is made by the MU-scheduler.

Each sector (BS or cell) m is equipped with a M-MIMO antenna with $N = N_x \times N_z$ radiating elements, and is serving N_m mobiles, each with one receiving antenna (the beam generation and antenna modeling is explained in details in [6]). Figure 1 presents the coverage area provided by GoBs of two adjacent cells for the case of $N_x = N_z = 16$. The color code is used to simplify visualization and has no physical meaning. Fading is removed for clarity. It is noted that the zeros of the beam radiation patterns in the azimuth axis close to the BSs is due to the zeros in the beam radiation patterns and the fact that reflections and fading are not omitted. It is recalled that beams for control channels are activated one by one (via beam sweeping) whereas several beams for data channels can be scheduled simultaneously.

We consider two BSs (i.e. macro cells) m and m' which interfere each other, each of which having a GoB denoted by $\mathcal{B}_m$ and $\mathcal{B}_{m'}$ respectively as shown in Figure 1. We assume that a cell can serve up to K users in a time slot, with at most one user per beam b. The users are selected according to a PF criterion.

Assume that the BS serves k users at a given time slot with $k \leq K$ and denote by p_{max} the maximum transmission power of the BS. The power p_m that the BS m transmits to user u, equals $\frac{p_{max}}{k}$. Denote by $C_u^{m,b}$ the useful signal received power of user u from beam b of BS m, by $d_{u,m}$ - the distance between m and u, and by σ - the thermal noise. $C_u^{m,b}$ can be written as a function of the channel gain $h_{b_u}^m(u)$:

$$C_u^{m,b} = p_m|h_b^m(u)|^2. \qquad (1)$$

$|h_{b_u}^m(u)|^2$ is modeled as the product between the pathloss, the antenna gain $G_{b_u}^m(u)$ of the beam b_u serving

Fig. 1: GoBs of two neighboring cells projected on the surface

user u and measured at the direction of user u, and the fast fading term $Z(u)$. The latter is modeled as a realization (per user) of a Nakagami distribution, and can be parameterized for different propagation environment [7].

$$|h_{b_u}^m(u)|^2 = \frac{c}{d_{u,m}^\gamma} G_{b_u}^m(u)Z(u) \qquad (2)$$

where c and γ are constants that depend on the type of environment. The interference generated by a cell m' on u is written as the sum of interferences from its active beams $I_u^{b'}$:

$$I_u^{m'} = \sum_{b' \in \mathcal{B}_{m'}} I_u^{b'} \qquad (3)$$

where

$$I_u^{b'} = p_{m'} \sum_{u' \in b', u' \neq u} |h_{b'_{u'}}^{m'}(u)|^2 \qquad (4)$$

The Signal to Interference plus Noise Ratio (SINR) of a user u attached to cell m is written as:

$$S_u^m = \frac{p_m|h_{b_u}^m(u)|^2}{\sum\limits_{m'} I_u^{m'} + \sigma^2} \qquad (5)$$

A full buffer traffic model is assumed. The baseline scheduler is based on PF without coordination.

III. COORDINATED SELF-ORGANIZING SCHEDULING

A. Architecture framework

The architecture supporting the ANBR based coordination is shown in (Figure 2). A centralized ANBR SON function is deployed at the management and orchestration

plane as an application (but can be implemented in a distributed manner as well). It provides a static matrix $\mathbf{A}^{m,m'}$ for any two cells m and m', with elements $A^{m,m'}_{b,b'}$. For simplicity of notations we omit the superscripts m and m' from the matrix $\mathbf{A}$ in the rest of the sequel. $A_{b,b'} = 1$ if the beam b of cell m and beam b' of cell m' interfere each other (as mentioned in Section I), and 0 otherwise. The matrix $\mathbf{A}$ is calculated and updated (not often) according to the operator policy and is considered here as constant.

The Distributed Unit (DU) (i.e. Radio Link Control (RLC), Media Access Control (MAC) and Physical (PHY)-High control protocol stack), hosts a new functional block denoted in Figure 2 as D-ANBR. The D-ANBR receives and processes measurements from the Radio Units (RUs). It dynamically updates the beam relations' matrix $\mathbf{A}$ and keeps only those relations corresponding to the present traffic distribution (as described in the next subsection). The resulting sparser matrix, $\mathbf{Q}$, is transmitted to the schedulers of BSs m and m' and is used to coordinate them. The time scale for generating the matrix $\mathbf{Q}$ is that of the traffic dynamics, e.g. of the order of a second.

It is noted that the introduction of new control, Radio Resource Management (RRM) or machine learning algorithms is currently studied in different standardization fora. As an example, the ORAN Alliance is defining new interfaces and protocols to support deployment of such algorithms in different network nodes [8].
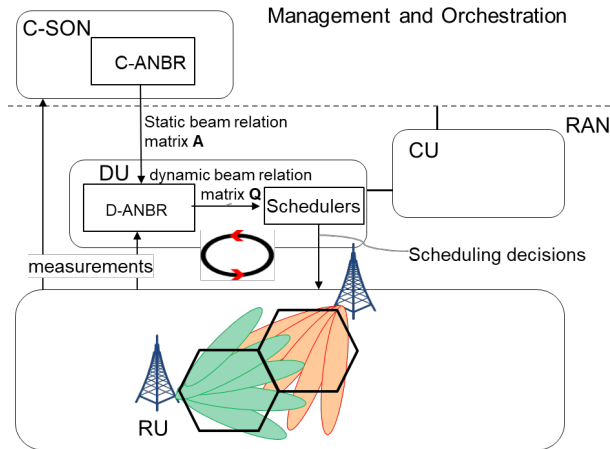

Fig. 2: System architecture

B. ANBR-assisted coordinated scheduling

We first describe the generation of the matrix $\mathbf{Q}$ and then explain how it is used to coordinate the MU schedulers of BSs m and m'.

Denote by $\mathcal{U}^{serv}_{b,m}$ the set of users served by beam b of BS m:

$$\mathcal{U}^{serv}_{b,m} = \{u \in m | b = \arg\max_{\bar{b} \in \mathcal{B}_m} C^{m,\bar{b}}_u\} \qquad (6)$$

We define two indicators used to generate the matrix $\mathbf{Q}$ using $\mathbf{A}$. The first, $\mathcal{A}_1(b, u')$, indicates whether user u' achieves low Signal to Interference Ratio (SIR) that is below a predefined threshold γ_{th} and is thus likely to experience strong interference from beam b:

$$\mathcal{A}_1(b, u') = \begin{cases} 1 & if \; \frac{C^{m'}_{u'}}{I^b_{u'}} < \gamma_{th} \\ 0 & otherwise \end{cases} \qquad (7)$$

For clarity of notation the beam b' serving user u' is not included in (7). Denote by $\mathcal{U}^{int}_b$ the set of users $u' \in m'$ for which $\mathcal{A}_1(b, u') = 1$, namely the set of users that could benefit the most from reducing the interference from beam b:

$$\mathcal{U}^{int}_b = \{u' \in m' | \mathcal{A}_1(b, u') = 1\}. \qquad (8)$$

The cardinality of $\mathcal{U}^{serv}_b$ and $\mathcal{U}^{int}_b$ are denoted by n^{serv}_b and n^{int}_b respectively,

$$n^{int}_b = |\mathcal{U}^{int}_b| \qquad (9)$$

$$n^{serv}_b = |\mathcal{U}^{serv}_b| \qquad (10)$$

The second indicator, $\mathcal{A}_2(b)$, is used to verify whether the ratio between the number of users that beam b interferes and the number of users it serves is above a threshold η_{th}. The rational is that the benefit from muting or limiting the allocated resources to a beam during a Transmission Time Interval (TTI) increases with the amount of users it interferes and decreases with the amount of users it serves.

$$\mathcal{A}_2(b) = \begin{cases} 1 & if \; \frac{n^{int}_b}{n^{serv}_b} > \eta_{th} \\ 0 & otherwise. \end{cases} \qquad (11)$$

The matrix element $Q_{b,b'}$ of $\mathbf{Q}$ is defined as follows:

$$Q_{b,b'} = A_{b,b'} \times 1_{\{\mathcal{A}_2(b)=1\}} \times 1_{\{\mathcal{A}_2(b')=1\}} \qquad (12)$$

The threshhold values of η_{th} and γ_{th} are determined using a simple optimization procedure (see details is Section IV).

The rationale for (12) is the following: consider the case where coordination is based on constraining the MU schedulers, namely not to schedule users served by beams b and b' in the same TTI for which $Q_{b,b'} = 1$ (see Algorithm 2). From eq. (12), the coordination is performed if both users served by b and b' will benefit from coordination, namely local QoS loss is avoided even

if globally performance is improved. The algorithm for generating the matrix **Q** is given by Algorithm 1.

Algorithm 1 Code Generation

Input: **A**
Init: **Q** =[0], matrix of the same dimension as **A**
for all couples (b, b') for which $A_{b,b'} = 1$ **do**
$\quad n_b^{int} \leftarrow |\mathcal{U}_b^{int}|, n_b^{serv} \leftarrow |\mathcal{U}_b^{serv}|$
$\quad n_{b'}^{int} \leftarrow |\mathcal{U}_{b'}^{int}|, n_{b'}^{serv} \leftarrow |\mathcal{U}_{b'}^{serv}|$
$\quad Q_{b,b'} = A_{b,b'} \times 1_{\{\mathcal{A}_2(b)\}} \times 1_{\{\mathcal{A}_2(b')\}}$
end for

The MU scheduling uses a known beam selection feature known as *beam skipping* technique that is applied independently in each cell. It allows to reduce intra- and inter-beam interference and to improve users' rates. It is noted that the ANBR based coordinated scheduling is independent of the beam skipping feature and can be applied without it. Each user is attached to the beam of the GoB achieving the best SINR. The user attachment provides certain spatial information that is exploited by the scheduler to mitigate interference: (i) by avoiding scheduling two users attached to the same control beam and (ii) by avoiding scheduling two users attached to adjacent beams of the GoB, both in the same TTI.

We first present a time based ANBR coordination scheme, denoted for sake of brevity as *time-ANBR* scheme. In this scheme, coordination is achieved by muting of certain beams during certain TTIs as explained below. For sake of simplicity, delay has been ignored but can be easily incorporated into the coordiation scheme.

Denote by $R_{u,t_{M+1}}^b$ the instantaneous rate of a user $u \in m$ when it is scheduled at t_{M+1}, by $\overline{R_{u,t_M}^b}$ - its average rate computed over a time window $[t_{M-T}, t_M]$, and by $d > 0$ a number chosen as small as possible. Denote by $\mathcal{U}_{candidates}$ the set of users that can still be scheduled and by $\mathcal{U}_K$ - the set of users already selected for scheduling, both at t_{M+1}.

Consider next the scheduling algorithm of cell m (or m') (see Algorithm 2). In the initialization phase, $\mathcal{U}_{candidates}$ contains all the users attached to m (or m'). The scheduler ranks the users in $\mathcal{U}_{candidates}$ with respect to a PF criterion, namely $\frac{R_{u,t_{M+1}}^b}{\overline{R_{u,t_M}^b} + d}$.

All beams $b \in \mathcal{B}_m$ for which $Q_{b,b'} = 1$ are muted at an even TTI, whereas the beams $b' \in \mathcal{B}_{m'}$ are muted at an odd TTI. The users of a muted beam are removed from $\mathcal{U}_{candidates}$. The scheduler selects the top-ranked candidate. Then, it removes the selected users attached to the adjacent beams from the candidate list (following the beam skipping scheme). We repeat the above two

operations until K candidates are selected or until the set of candidates is empty.

Algorithm 2 ANBR-assisted MU Scheduler

Input : **Q**
Init: $\mathcal{U}_K = \{\}, \mathcal{U}_{candidates} = \{u \in m\}$
if TTI is even **then**
$\quad$ **for all** b for which $Q_{b,b'} = 1$ **do**
$\quad\quad$ Remove $u \in b$ from $\mathcal{U}_{candidates}$
$\quad$ **end for**
end if
while $|\mathcal{U}_k| < k$ **or** $\mathcal{U}_{candidates} \neq \emptyset$ **do**
$\quad u_{select} \leftarrow \text{argmax}_{u \in \mathcal{U}_{candidates}} \frac{R_{u,t_{M+1}}^b}{\overline{R_{u,t_M}^b} + d}$
$\quad \mathcal{U}_k \leftarrow \mathcal{U}_k \cup u_{select}$
$\quad$ Remove users attached to the beam of u_{select} and to the adjacent beams from $\mathcal{U}_{candidates}$
end while

The second coordination scheme is denoted as frequency based ANBR coordination scheme and is denoted for sake of brevity as *frequency-ANBR* scheme. This scheme is similar to the time-ANBR namely instead of consecutively muting beams for which $Q_{b,b'} = 1$, we allocate to these beams half of the available non-overlapping resources. It is noted that in spite of being very simple, both time- and frequency-ANBR coordination schemes achieve high performance with little computational efforts.

Lastly, the generalization of the coordinated scheduling to the case where beams from three cells interfere with each other is straightforwards. Sparse three dimensional matrices **A** and **Q** need to be generated, and non-overlapping resources (e.g. Physical Resource Blocks (PRBs) in the frequency-ANBR) should be allocated to the beams. One should bare in mind that significant co-located interference from several cells should be minimized in the cell-planning phase and not by the scheduler.

IV. NUMERICAL RESULTS

A. Simulation scenario

Consider a network comprising 19 sectors (cells): a central sector and two tiers of 18 neighboring sectors (6 sites located on a hexagonal grid) surrounding it. Each base station is equipped with a M-MIMO antenna as described in Section II. The central sector and one of its direct neighbors denoted hereafter as cell 1 and cell 2 (respectively upper left and lower right in Figure 1), implement the coordinated scheduling. The reference scenario with no coordination serves as a baseline. It implements a PF based MU-scheduler with the beam

skipping feature. Both the time- and frequency-based ANBR coordinated scheduling are simulated and compared to the baseline scenario. The simulation parameters are summarized in Table I.

TABLE I: Network and Traffic characteristics

Network parameters	
Number of BSs	2
Number of interfering macros	6x3 sectors
Macro-cell layout	Hexagonal trisector
Number of beams b per macro cell	16
Bandwidth	20 MHz
Channel characteristics	
Thermal noise	-174 dBm/Hz
Path Loss (d in km)	128.1 + 37.6 $\log_{10}(d)$ dB
Nakagami-m shape parameter	5
Intersite distance	500 m
Traffic characteristics	
Number of user in the hotspot zone of each cell	35
Number of user outside the hotspot zone in each cell	10
Traffic distribution in hotspot zone	Uniform
Traffic distribution outside hotspot zone	Uniform
Service Type	Full buffer, data

The traffic distribution of cells 1 and 2 is shown in Figure 4. A red rectangle surrounds a hotspot zone with high traffic located around the cell edge area of the two cells. Each cell has 35 users in the hotspot area and 10 users in the rest of the cell, drawn according to a uniform distribution in each zone. The users' color code in Figure 4 is the following: red and blue squares are the users outside of the hotspot and belonging to the cell 1 and 2 respectively, green and yellow are the users of cell 1 and 2 located in the hotspot.

The best values for the thresholds η_{th} and γ_{th} are determined by means of an exhaustive search. We define a uniform grid of 10×10 points (η_{th},γ_{th}), with η_{th} varying from $1/10$ to 1 and γ_{th} - from 1 to 10. For each point of the grid we compute the Mean User Throughput (MUT) gain using the time-ANBR coordination scheme as depicted in Figure 3. The gain increases with the decrease in η_{th} while the MUT gain is not sensitive to variations in γ_{th} except for small values. Too small value of γ_{th} results in too few mobiles that can benefit from the coordination between the two cells. Similarly, a small value of η_{th} allows more beam relations to be included in the matrix **Q** and more users will participate in the coordinated scheduling. In the rest of the paper, the thresholds' values of $\gamma_{th} = 2.5$ and $\eta_{th} = 1/6$ are set. A gain of 105% in MUT with respect to the baseline is achieved on a plateau of 27 points, indicating little sensitivity of the thresholds (see Figure 3).

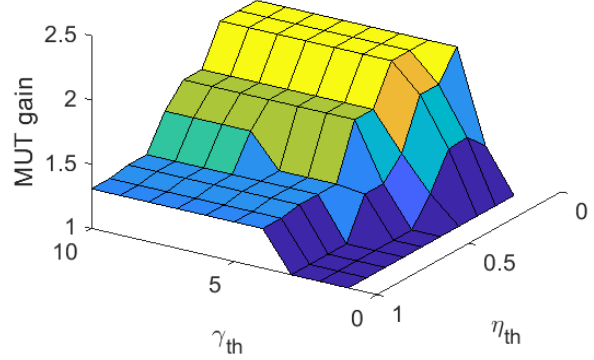Figure 5 presents the distribution of the served - and

Fig. 3: Comparison of MUT as a function of the thresholds γ_{th} and η_{th}

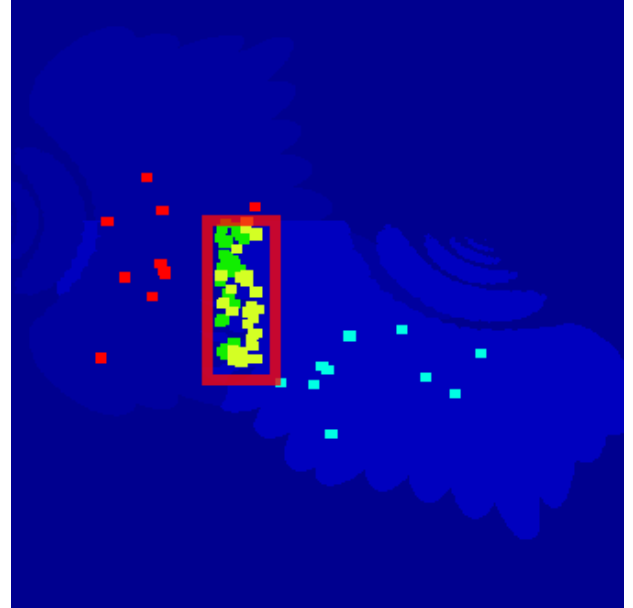interfered users per beam for both cells using equations (10) and (9) respectively.

Fig. 4: Traffic map

B. Performance analysis

Figures 6 and 7 compare MUT results for the two coordination schemes, the time- and frequency-ANBR and the baseline. The average results per cell are depicted in Figure 6 and the time evolution of the MUT for both cells is shown in Figure 7. The improvement brought about by the coordination schemes is very significant, of the order of 100%. One can see that the time-ANBR performs a
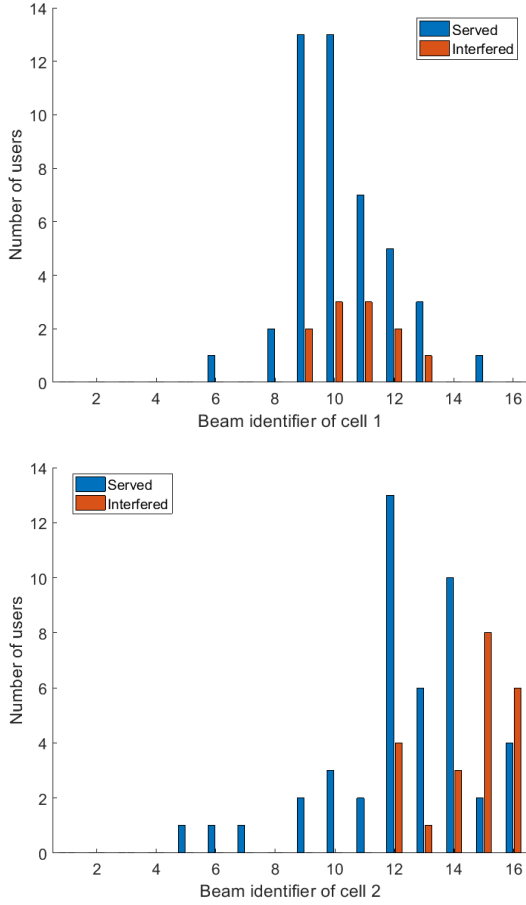
Fig. 5: Number of served and interfered users per beam

Fig. 6: MUT for frequency(in red)- and time(in yellow)-ANBR and baseline(in blue)

Fig. 7: Time evolution of the MUT of the network

bit better than the frequency-ANBR based coordination. This is explained by the fact that when a beam is muted, time resources will be used by users served by other beams. In the case of frequency-ANBR, the coordinated beams are allocated non-overlapping frequency resources and hence not all the available resource are used.

In the following results, we consider the frequency-ANBR coordination scheme compared to the baseline. We divide the users into two groups as a function of their locations, namely outside and inside the hotspot area. The users' throughput are presented in the form of horizontal bars, in an increasing order of throughput values in the baseline case (in blue). The same order is kept for the coordinated scheduling case (in red) to ease comparison.

Figures 8 and 10 present the throughputs of the users outside the hotspot zone of cells 1 and 2 respectively. In cell 1 (8) certain users see their throughput grows significantly since they benefit from the cells coordina-
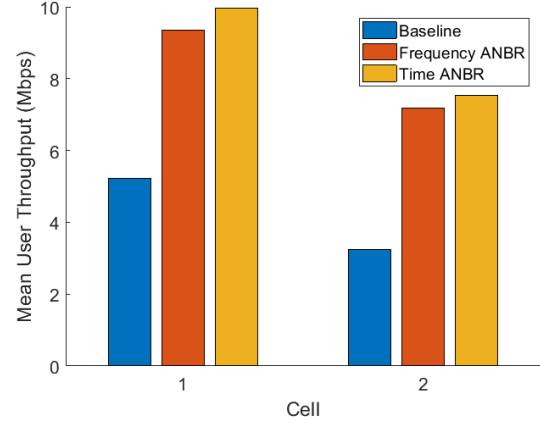
tion, while other users see their throughputs slightly decreased. In cell 2 (Figure 10) a non-significant throughput reduction is observed.

Figures 9 and 11 show the throughputs of the users in the hotspot area of cells 1 and 2 respectively. One can clearly see that most of the users benefit from the coordinated scheduling and see their throughputs significantly increased.
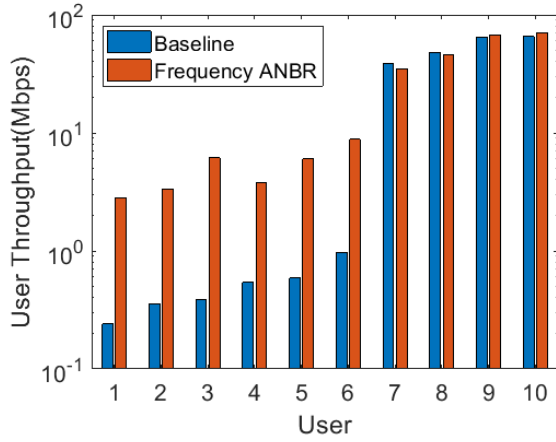
Fig. 8: Throughputs of users outside the hotspot zone in cell 1
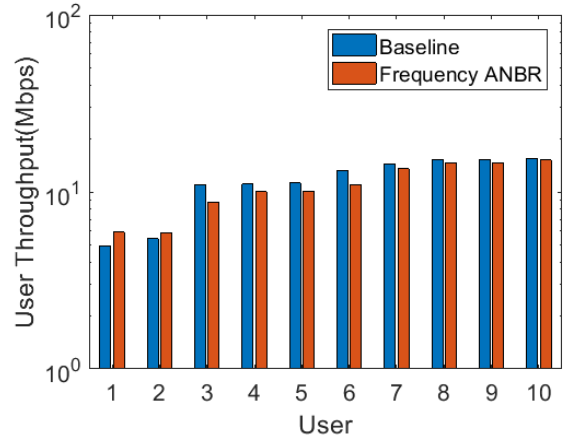

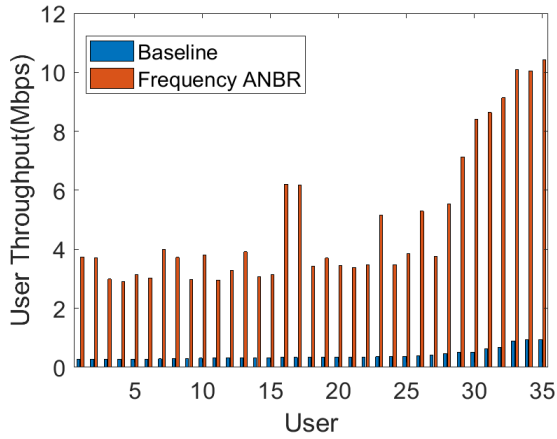Fig. 10: Throughputs of users outside the hotspot zone in cell 2

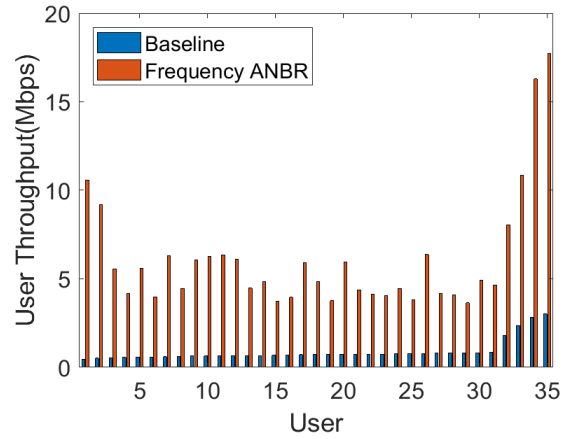Fig. 9: Throughputs of users in the hotspot zone in cell 1

Fig. 11: Throughputs of users in the hotspot zone in cell 2

V. CONCLUSION

This paper has shown how ANBR can be used to coordinate MU scheduling of a pair of neighboring cells with M-MIMO deployment. The strong interference at cell edge motivates the coordination approach. Two solutions have been proposed, a time- and a frequency based coordinated scheduling. The coordination solution exploits the capability to derive beam relations of neighboring cells, which is supported by 5G technology. The beam relations are updated at the time scale of arrival and departure of users, namely in the order of a second. It makes this approach attractive with respect to traditional techniques such as CoMP which operates at a millisecond time scale and requires high processing capabilities. The coordinated scheduling solution brings about significant throughput gains to users located close to cell edge or in highly interfered area. The ANBR feature has an important potential for other resource allocation and optimization problems such as mobility or load balancing.

REFERENCES

[1] Björnson *et al.*, "Massive MIMO networks: Spectral, energy, and hardware efficiency," *Foundations and Trends® in Signal Processing*, vol. 11, no. 3-4, pp. 154–655, 2017.

[2] F. W. Vook *et al.*, "MIMO and beamforming solutions for 5G technology," in *2014 IEEE MTT-S International Microwave Symposium (IMS2014)*, 2014, pp. 1–4.

[3] P. Ramachandra *et al.*, "Automatic neighbor relations (ANR) in 3GPP NR," in *IEEE Wireless Communications and Networking Conference Workshops (WCNCW)*, 2018, pp. 125–130.

[4] A. Dahlen *et al.*, "Evaluations of lte automatic neighbor relations," in *2011 IEEE 73rd Vehicular Technology Conference (VTC Spring)*, 2011, pp. 1–5.

[5] R. Irmer *et al.*, "Coordinated multipoint: Concepts, performance, and field trial results," *IEEE Communications Magazine*, vol. 49, no. 2, pp. 102–111, 2011.

[6] A. Tall *et al.*, "Multilevel beamforming for high data rate communication in 5G networks," *arXiv preprint arXiv:1504.00280*, 2015.

[7] U. Charash, "Reception through Nakagami fading multipath channels with random delays," *IEEE Transactions on Communications*, vol. 27, no. 4, pp. 657–670, 1979.

[8] O-RAN Alliance, "O-RAN:towards an open and smart ran," *White Paper*, 2018.